DOI: 10.1002/ejic.200500495

Synthetic, Structural, and Electrochemical Studies of 2-Ferrocenyl- and 2-Cymantrenyl-Functionalized 2,3-Dihydro-1*H*-1,3,2-diazaboroles and 1,3,2-Diazaborolidenes

Lothar Weber,*[a] Imme Domke,[a] Hans-Georg Stammler,[a] and Beate Neumann[a]

Keywords: Boron / Cyclic voltammetry / Ferrocene / Methylcymantrene

Reaction of (dibromoboryl)ferrocene (**1**) with 1 equiv. of the diazabutadiene *t*BuN=CH–CH=N*t*Bu, and subsequent reduction of the obtained borolium salt **2** with sodium amalgam, affords the first ferrocenyl-functionalized 1,3,2-diazaborole (**3**). Similarly, 1,1′-bis(dibromoboryl)ferrocene (**4**) can be transformed into compound **6**, which contains two diazaborolyl substituents at the ferrocene core. Treatment of precursors **1** and **4** with 1,2-bis(*tert*-butylamino)ethane in the presence of Et_3N gives rise to the formation of the diazaborolidine derivatives **13** and **14**. 1-Dibromoboryl-3-methylcymantrene (**7**) was also treated with *t*BuN=CH–CH=N*t*Bu to give the borolium salt **8**, which was subsequently reduced to the 2-cymantrenyl-diazaborole **9**. Treatment of **7** with *t*BuN(H)-CH_2CH_2N(H)*t*Bu in the presence of Et_3N furnished the corresponding 2-cymantrenyl-diazaborolidine **15**. The novel compounds were characterized by elemental analyses and various spectroscopic techniques (IR; ^{1}H, ^{13}C, and ^{11}B NMR; MS). The molecular structures of **3**, **6**, and **15** were elucidated by X-ray diffraction analyses. Cyclovoltammetric studies of the ferrocene derivatives at high scan rates show features of a quasireversible oxidation at the iron center. The heterocyclic groups serve as electron donors, considerably lowering the oxidation potential of the central iron atoms when compared to the parent compound ferrocene.

Introduction

Boryl- and borate-functionalized metallocenes are of great current interest. Two recent reviews have described their applications in homogeneous catalysis, anion sensing, and organometallic polymer chemistry.[1,2] Another point of interest is related to the influence of the boryl substituent on the electronic and structural properties of the metallocene moiety. The boron systems that concern us are 2,3-dihydro-1*H*-1,3,2-diazaboroles **A**, for which we have recently developed high-yield syntheses.[3] With this, the door was opened to an exceedingly rich chemistry of these heterocycles, including reactions where the structural integrity of the ring system is retained (e.g. nucleophilic displacements at the boron atom)[4] as well as processes where the ring is reorganized (e.g. in the reaction with diphenylketene to afford 1,3,2-oxazaborolidenes **B**;[5] Scheme 1).

At this point, it was of particular interest to combine such inorganic heterocycles with metallocene fragments. It is conceivable that the 6π-electron-containing heterocycle communicates electronically with the metallocene by (pp)π-interactions and/or σ-bonding, thus altering the electronic properties of the organometallic moiety.

In this paper we report on the synthesis and molecular structures of ferrocenyl- and cymantrenyl-functionalized 1,3,2-diazaboroles as well as their saturated counterparts, the respective 1,3,2-diazaborolidines. Moreover, electrochemical studies should provide information on the influence of the boron heterocycles on the redox-active center of the organometallic fragment.

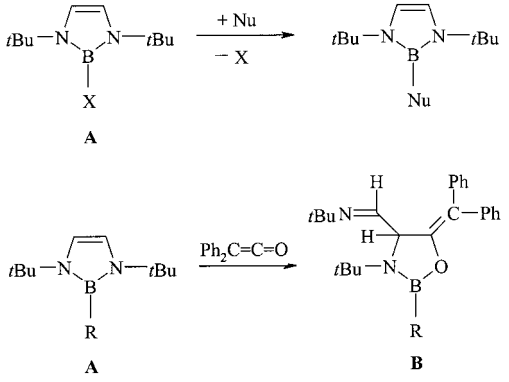

Scheme 1. Reactivity of 1,3,2-diazaboroles **A**.

Results and Discussion

Several synthetic pathways for the construction of the 2,3-dihydro-1*H*-1,3,2-diazaborole system are currently available:

a) the catalytic dehydrogenation of the corresponding saturated 1,3,2-diazaborolidines;[6]

[a] Fakultät für Chemie der Universität Bielefeld,
Universitätsstraße 25, 33615 Bielefeld, Germany
Fax: +49-521-106-6146
E-mail: lothar.weber@uni-bielefeld.de

b) the reaction of di- or trihaloboranes with 1,4-diazabutadienes to afford borolium salts and the reduction of the latter species with sodium amalgam;[4,7]
c) the cyclocondensation of di- and trihaloboranes with dilithiated diazabutadienes;[4] and
d) nucleophilic substitution processes at the boron atom of preformed 2-halo-1,3,2-diazaboroles[4] (Scheme 2).

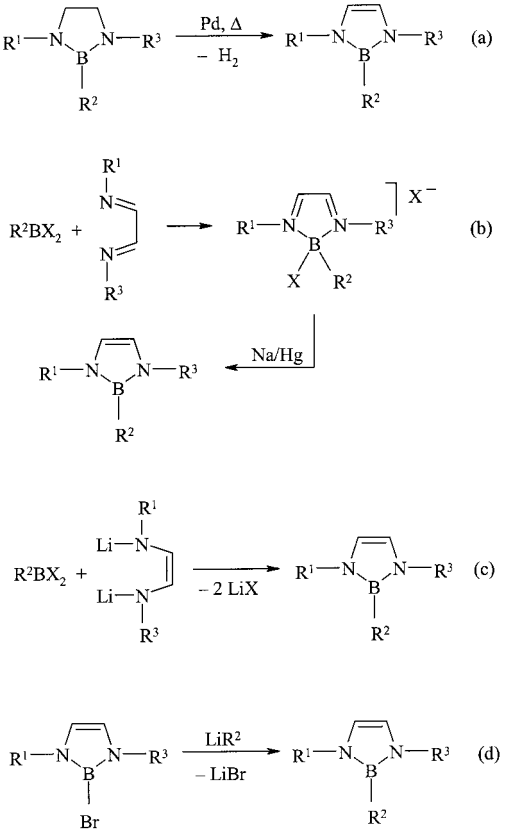

Scheme 2. Synthethic pathways to 1,3,2-diazaboroles.

Path (b) seems promising for the synthesis of 2-ferrocenyl- and 2-(methylcymantrenyl)-functionalized diazaboroles as the required precursors (dibromoboryl)ferrocene (**1**), 1,1′-bis(dibromoboryl)ferrocene (**4**), and 1-dibromoboryl-3-methylcymantrene (**7**) are readily available from ferrocene and methylcymantrene by Friedel–Crafts-type reactions with BBr_3 (Scheme 3).[8]

Reaction of **1** with the diazabutadiene (tBuN=CH)$_2$[9] in n-hexane gave an olive-green precipitate of borolium salt **2**, which shows resonances in the $^{11}B\{^1H\}$ NMR spectrum in the region of tetracoordinate boron [δ = 3.8, 7.1 ppm (CD_3CN)]. The two different signals are presumably due to different counterions in the salts. This phenomenon has frequently been encountered during the synthesis of borolium salts from diazabutadienes and boron halides.[4c,10] The obtained slurry was reduced in situ with an excess of sodium amalgam for2 d in the absence of light. Red crystals of product **3** were isolated in 74% yield from the resulting dark-red n-hexane phase. Similarly, the treatment of 1,1′-bis(dibromoboryl)ferrocene with2 equiv. of diazabutadiene gave borolium salt **5** [$\delta_{^{11}B}$ = 3.8, 7.1 ppm (CD_3CN)], which

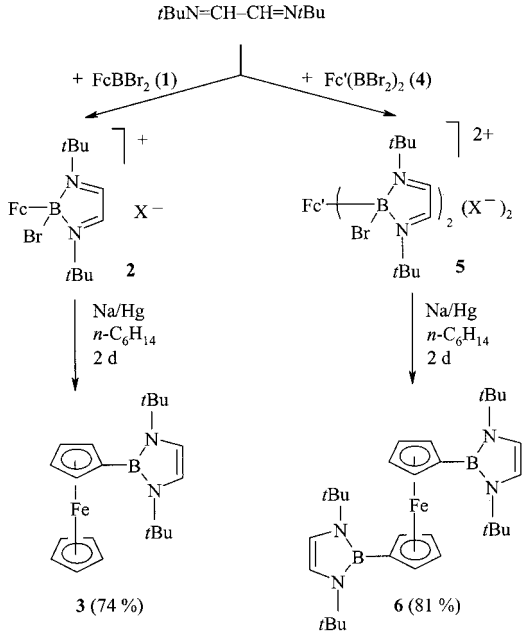

Scheme 3. Syntheses of **3** and **6** {Fc = [(C_5H_5)(C_5H_4)Fe]; Fc′ = [(C_5H_4)$_2$Fe]; X = Br}.

was subsequently reduced to bis(borolyl)ferrocene **6**. The product was isolated as cherry-red crystals in 81% yield (Scheme 3).

Yellow, crystalline methylcymantrenyl-1,3,2-diazaborole (**9**) was synthesized in 63% yield by the reaction of complex **7** with the diazabutadiene in n-hexane and the usual reduction of the borolium salt [$\delta_{^{11}B}$ = 5.0 ppm (CD_3CN)] with sodium amalgam (Scheme 4).

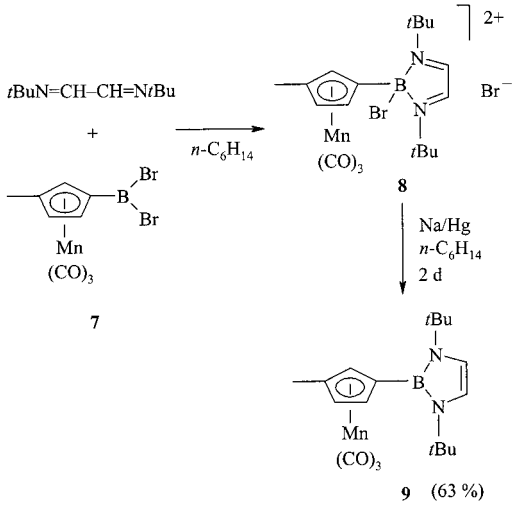

Scheme 4. Synthesis of **9**.

Thermolabile 2-ferrocenyl[1,3,2]diazaborolo[1,5-*a*]pyridine (**11**) was accessible by treatment of **1** with *N*-(2-pyridylmethylene)-*tert*-butylamine[11] and the subsequent reduction of borolium salt **10** ($\delta_{^{11}B}$ = 6.3, 7.8 ppm) to produce the orange solid product (Scheme 5).

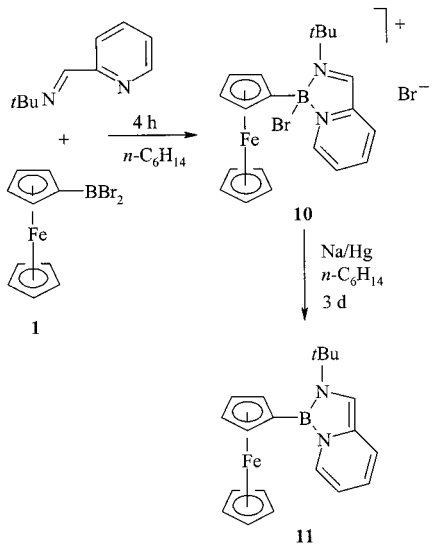

Scheme 5. Synthesis of **11**.

For comparison, the saturated analogs of the organometallic diazaboroles **3**, **6**, and **9** − the respective 1,3,2-diazaborolidenes − were also studied. One complex of this type, compound **12**, has previously been synthesized by the reaction of 1,1′-dilithioferrocene with 2-chloro-1,3-dimethyl-1,3,2-diazaborolidine.[12]

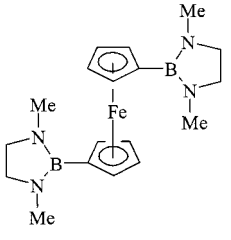

In this study, the aminolysis of the B–Br bonds in **1**, **4**, and **7** by *N*,*N*′-di-*tert*-butylethane-1,2-diamine in the presence of triethylamine was preferred as a synthetic approach (Scheme 6).

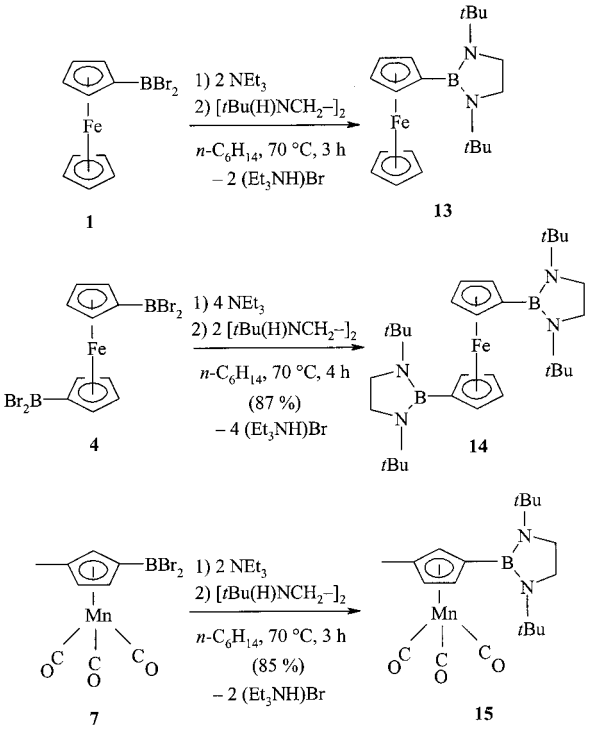

Scheme 6. Synthesis of diazaborolidines **13**–**15**.

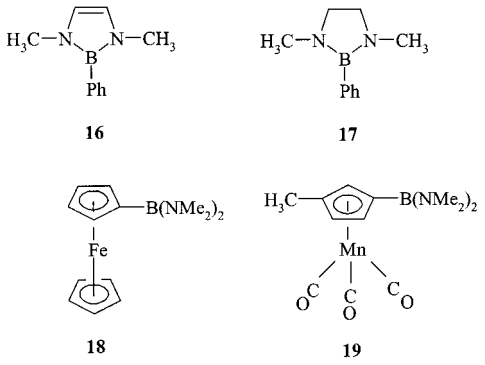

The reactions were performed in boiling *n*-hexane for 3–4 h to afford red, oily **13**, dark-red, crystalline **14**, and colorless, crystalline **15** in good yields (85–87%). All the novel organometallic diazaboroles and diazaborolidines are sensitive to air and moisture. Moreover, the thermolability of compound **11** precluded reliable elemental analyses.

The $^{11}B\{^1H\}$ NMR spectra of the ferrocenyl-diazaboroles **3** and **6** display resonances at δ = 25.3 ppm, which are comparable with the ^{11}B NMR signal of 2-phenyl-1,3,2-diazaborole (**16**; δ = 25.6 ppm).[6] Generally, the shielding of the ^{11}B nuclei in 1,3-dialkyl-1,3,2-diazaboroles is mainly governed by the substituents at the boron atom.

This resonance is shifted by 6.5 ppm to δ = 31.8 ppm on going to the saturated systems **13** and **14**. Again, these resonances compare well with the ^{11}B NMR signal of 1,3-dimethyl-2-phenyl-1,3,2-diazaborolidine (**17**; δ = 32.2 ppm).[6] The ^{11}B NMR signal in the acyclic (diaminoboryl)ferrocene **18** appears at δ = 33.3 ppm,[8b] thus indicating that the ferrocenyl and the phenyl group at the boron atom contribute similarly to the shielding of the boron center. The situation is similar in the ^{11}B NMR spectra of the methylcymantrenyl derivatives. In the methylcymantrenyl-substituted diazaborole **9**, for example, the ^{11}B NMR resonance is observed at δ = 23.2 ppm. The ^{11}B atom of diazaborolidine **15** is more deshielded (δ = 29.6 ppm) as in the corresponding 6π-electron heterocycle. The ^{11}B NMR signal of the acyclic bis(aminoboryl) derivative **19** appears at δ = 30.1 ppm.[8b]

The chemical shifts of the ^1H and ^{13}C nuclei of the C_5H_5 ring in monoborylated ferrocenes in comparison to the parent compound is thought to reflect the donor/acceptor properties of the boryl substituent. Thus, on going from $[FeCp_2]$ ($\delta_{^{13}C}$ = 68.2 ppm) to the dibromoboryl derivative **1** ($\delta_{^{13}C}$ = 71.7 ppm) this resonance is shifted by 3.5 ppm. In comparison, the 1,3,2-diazaborolyl- and 1,3,2-diazaborolidinyl substituents in **3** and **13** (δ = 69.6 ppm) give rise to

the considerably smaller low-field shift of only 1.4 ppm. In ferrocene **18**, which contains the $B(NMe_2)_2$ group as a substituent, a singlet is observed at $\delta_{^{13}C}$ = 68.6 ppm. The signals of the α- and the β-C atoms of the C_5H_4B unit in **1** are found at $\delta_{^{13}C}$ = 77.4 and 78.4 ppm, respectively, whereas the corresponding signals in the bis(dibromoboryl)ferrocene **4** appear at δ = 79.0 and 80.3 ppm. In the monoborolyl- and monoborolidinyl ferrocenes **3** and **13** the nuclei $^{13}C_\alpha$ and $^{13}C_\beta$ resonate at δ = 76.2, 68.6 (**3**) and 76.2, 68.3 (**13**) ppm. For comparison, the corresponding signals in **18** appear at $\delta_{^{13}C}$ = 76.0 and 70.1 ppm.[12] The resonances for the $^{13}C_\alpha$- and $^{13}C_\beta$ atoms of the diborylated species **6** and **14** are found at $\delta_{^{13}C}$ = 79.3 (**6**) and 79.0 (**14**), and 68.6 (**6**) and 68.3 (**14**) ppm. The pronounced difference in the resonances of C_α and C_β in **3**, **6**, **13**, **14**, and **18** agrees with a significant transfer of negative charge from the heterocycles to the organometallic unit via the B–C σ-bond. Singlets at δ = 112.7 or 112.9 ppm in the ^{13}C NMR spectra of **3** and **6**, respectively, were assigned to the C=C groups of the diazaborole.

The ^1H NMR spectra of complexes **1**, **3**, **13**, and **18** show singlets in the narrow range of δ = 4.06–4.12 ppm for the C_5H_5 groups. The electron-withdrawing effect of one or two Br_2B units in **1** and **4** is reflected by the separation of the multiplets for H_α and H_β of the substituted rings by $\Delta\delta$ = 0.35 and 0.20 ppm, respectively, with δ_{H_β} at lower field. No such separation is observable in the monoborylated complexes **3**, **14**, and **18**, and in the diborylated ferrocenes **6** and **14** a separation of signals of only $\Delta\delta$ = 0.11–0.14 ppm is found. Singlets in the ^1H NMR spectrum of **9** at δ = 1.34 (18 H), 1.56 (3 H), 4.04 (1 H), 4.57 (1 H), 4.65 (1 H), and 6.34 (2 H) ppm are attributed to the protons of the *tert*-butyl groups, the ring methyl group, the protons H(4), H(2), and H(5) of the methylcyclopentadienyl ligand, and to the CH=CH unit, respectively. The corresponding resonances in the borolidinyl derivative **15** are found at δ = 1.30 (18 H), 1.68 (3 H), 4.14 (1 H), 4.64 (1 H), and 4.68 (1 H) ppm, whereas the protons of the CH_2–CH_2 fragment are observed as a singlet at δ = 3.11 ppm (4 H). The ^{13}C NMR spectra of **9** and **15** show singlets for the CO ligands at δ = 226.2 and 226.0 ppm, respectively, which are close to the resonance in methylcymantrene [δ(CO) = 225.7 ppm]. The ^{13}C NMR signals of the η^5-ligand in **9** and **15** are similar to those of **7**, where the Br_2B group is clearly electron-withdrawing. Here, singlets for C(3), C(5), C(2), and C(4) are found at δ = 107.2, 96.6, 95.8, and 90.0 ppm. In **9**, the respective resonances appear at δ = 99.8, 95.2, 94.8, and 90.0 ppm, which points to a higher electron density in the ring than in **7**. This tendency is even more pronounced in **15**, where singlets are observed at δ = 98.8, 94.1, 93.5, and 81.7 ppm. This is also mirrored in the ν(CO) region of the IR spectra of **7**, **9**, **15**, and $[(CH_3C_5H_4)Mn(CO)_3]$ (Table 1).

Two strong ν(CO) bands are observed at $\tilde{\nu}$ = 2025 and 1944 cm^{-1} due to the local C_{3v} symmetry of the $Mn(CO)_3$ group in the starting material. Strong absorptions at $\tilde{\nu}$ = 2020 and 1938 cm^{-1} in the spectra of **9** and **15**, respectively, show the transfer of electron density from the heterocyclic substituents to the carbonyl groups. In comparison to that, ν(CO) bands are found at higher wavenumbers for the dibromoboryl precursor **7** ($\tilde{\nu}$ = 2033, 1949 cm^{-1}) than for methylcymantrene.

Table 1. IR data of the methylcymantrene derivatives in *n*-hexane solutions.

Compound	$[(CH_3C_5H_4)Mn(CO)_3]$	**7**	**9**	**15**
$\tilde{\nu}$ [cm^{-1}]	2025, 1944	2033, 1949	2020, 1938	2020, 1938

X-ray Structural Analysis of 3, 6, and 15

X-ray analyses of compounds **3**, **6**, and **15** were carried out to determine the mutual orientation of the 1,3,2-diazaborolyl substituent and the η^5-C_5H_4 ring ligand, and for an evaluation of a possible π-conjugation between these cycles in the solid state (Table 3).

X-ray Structural Analysis of 3

An ORTEP drawing of **3** is shown in Figure 1; selected bond lengths and angles are given in the caption.

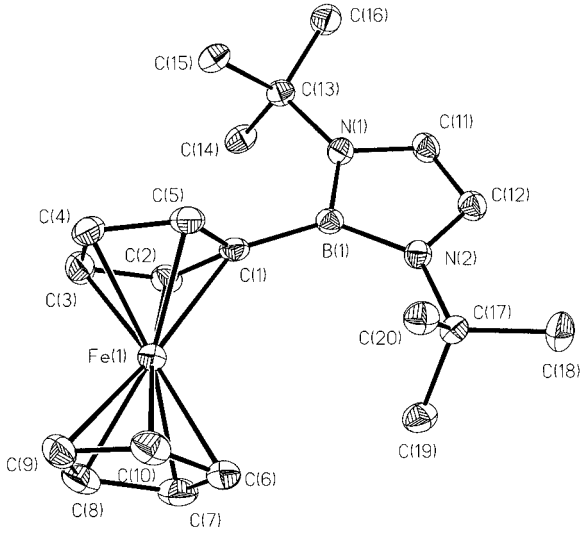

Figure 1. Molecular structure of **3** in the crystal. Selected bond lengths [Å] and angles [°]: B(1)–C(1) 1.588(2), B(1)–N(1) 1.455(2), B(1)–N(2) 1.444(2), N(1)–C(11) 1.400(2), N(2)–C(12) 1.396(2), N(1)–C(13) 1.497(2), N(2)–C(17) 1.488(2), C(11)–C(12) 1.342(2), Fe(1)–C(1) 2.132(2), Fe(1)–C(2) 2.053(2), Fe(1)–C(3) 2.031(2), Fe(1)–C(4) 2.038(2), Fe(1)–C(5) 2.066(2), Fe(1)–C(6,-10) 2.048(2)–2.070(2), C(1)–C(2) 1.434(2), C(2)–C(3) 1.421(2), C(3)–C(4) 1.424(3), C(4)–C(5) 1.426(2), C(1)–C(5) 1.437(2); N(1)–B(1)–N(2) 104.84(13), B(1)–N(1)–C(11) 107.21(13), N(1)–C(11)–C(12) 110.16(14), C(11)–C(12)–N(2) 109.75(14), B(1)–N(2)–C(12) 107.99(13), C(1)–B(1)–N(2) 133.04(15), C(1)–B(1)–N(1) 122.12(13), B(1)–N(2)–C(17) 130.51(13), B(1)–N(1)–C(13) 132.59(13), C(13)–N(1)–C(11) 120.19(13), C(12)–N(2)–C(17) 121.49(12), B(1)–C(1)–C(2) 124.81(14), B(1)–C(1)–C(5) 126.58(14), C(2)–C(1)–C(5) 105.24(14).

The molecular structure of **3** features a planar 1,3,2-diazaborole ring with a ferrocenyl substituent that is linked to the boron atom by a B–C single bond of 1.588(2) Å. This

value compares well with the B–C bond in the borolylimidazolium ion **20** [1.580(11) Å].[4d]

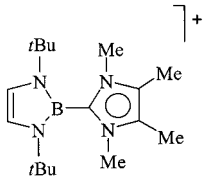

20

The atomic distances and valence angles are in good agreement with the equivalent data for cation **20**. The B–N bond lengths in **3** [1.444(2), 1.455(2) Å] indicate multiple-bond character. The B–N bond lengths in a series of diazaboroles range from 1.407(3) to 1.450(2) Å. The atomic distance C(11)–C(12) [1.342(2) Å] and the N–C(sp^2) bond lengths [1.396(2) and 1.400(2) Å] also indicate multiple bonding. Bond lengths of 1.497(2) and 1.488(2) Å are found for the N(sp^2)–C(sp^3) single bonds N(1)–C(13) and N(2)–C(17), respectively. The endocyclic angles in **3** [N(1)–B(1)–N(2) = 104.84(13)°, B(1)–N(1)–C(11) = 107.21(13)°, B(1)–N(2)–C(12) = 107.99(13)°, N(1)–C(11)–C(12) = 110.16(14)°, and N(2)–C(12)–C(11) = 109.75(14)°] resemble those in **20** [107.1(6), 105.9(4), and 110.5(3)°]. The exocyclic angle C(1)–B(1)–N(2) is much wider [133.04(15)°] than the C(1)–B(1)–N(1) angle of only 122.12(13)°, presumably due to severe steric interaction between the *tert*-butyl group at N(2) and the ferrocenyl unit. In the ferrocenyl part of the molecule it is obvious that the Fe(1)–C(1) bond of 2.132(2) Å significantly exceeds the distances between the metal atom and the remaining ring carbon atoms [2.031(2)–2.066(2) Å]. The Fe–C distances to the C_5H_5 ligand range from 2.048(2) to 2.070(2) Å, and the planes of the two Cp rings form an angle of 9.8°. The boron atom is not coplanar with ring C(1) to C(5), but is located 0.49 Å above this plane. The vector B(1)–C(1) and the ring plane enclose an angle of 17.6°. The diazaborole ring and the ring C(1) to C(5) form an angle of 73.1°, thus excluding significant π-communication between the two units.

X-ray Structural Analysis of 6

The molecular structure of **6** (Figure 2, Table 3) features a ferrocene scaffold, with each ring substituted by a planar 1,3,2-diazaborolyl group by single bonds [B(1)–C(11) = 1.596(3) Å; B(2)–C(16) = 1.584(4) Å].

The two cyclopentadienyl rings are not parallel but are bent by an angle of 12.9°. The heterocycle defined by the atoms B(1), N(1), N(2), C(1), and C(2) and the ring C(11)–C(15) show an interplanar angle of 46.6°. The plane of the second diazaborolyl substituent and the plane defined by the atoms C(16) to C(20) feature an interplanar angle of 103.1°. The boron atoms B(1) and B(2) are located 0.31 and 0.51 Å above their respective cyclopentadienyl ligands, which means that the vectors B(1)–C(11) and B(2)–C(16) form angles of 10.7° and 18.1° with the respective C_5H_4 planes. The vectors B(1)–C(11) and B(2)–C(16) form an angle of 75.7°, which mirrors a *gauche* conformation of both substituents. As already observed with complex **3**, the

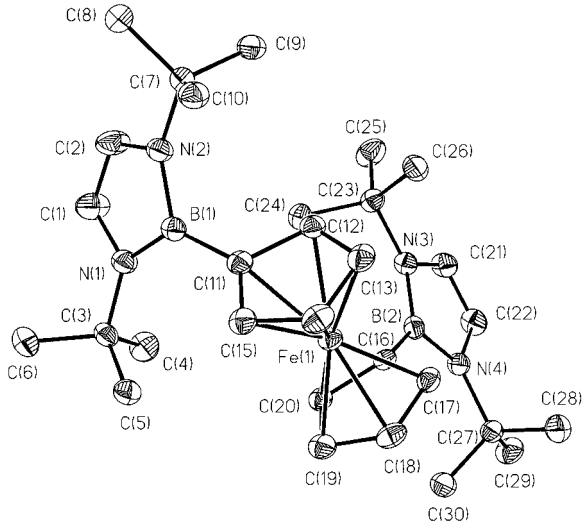

Figure 2. Molecular structure of **6** in the crystal. Selected bond lengths [Å] and angles [°]: B(1)–C(11) 1.596(3), B(1)–N(1) 1.450(3), B(1)–N(2) 1.464(3), N(1)–C(1) 1.396(3), N(1)–C(3) 1.485(3), N(2)–C(2) 1.379(3), N(2)–C(7) 1.499(3), C(1)–C(2) 1.343(3), B(2)–C(16) 1.584(4), B(2)–N(3) 1.447(3), B(2)–N(4) 1.462(3), N(3)–C(21) 1.404(3), N(3)–C(23) 1.483(3), N(4)–C(22) 1.397(3), N(4)–C(27) 1.497(3), Fe(1)–C(11) 2.136(2), Fe(1)–C(12) 2.051(2), Fe(1)–C(13) 2.044(2), Fe(1)–C(14) 2.042(2), Fe(1)–C(15) 2.072(2), Fe(1)–C(16) 2.155(2), Fe(1)–C(17) 2.059(2), Fe(1)–C(18) 2.026(2), Fe(1)–C(19) 2.035(2), Fe(1)–C(20) 2.079(2), C–C(Cp) 1.407(3)–1.436(3); B(1)–N(1)–C(1) 106.9(2), N(1)–C(1)–C(2) 110.4(2), N(2)–C(2)–C(1) 110.3(2), B(1)–N(2)–C(2) 107.3(2), N(1)–B(1)–N(2) 104.8(2), N(1)–B(1)–C(11) 132.8(2), N(2)–B(1)–C(11) 122.2(2), B(1)–N(1)–C(3) 135.7(2), C(1)–N(1)–C(3) 117.3(2), C(2)–N(2)–C(7) 118.0(2), B(1)–N(2)–C(7) 134.6(2), B(1)–C(11)–C(15) 132.5(2), B(1)–C(11)–C(12) 121.7(2), C(12)–C(11)–C(15) 104.7(2), B(2)–N(3)–C(21) 107.6(2), N(3)–C(21)–C(22) 110.2(2), N(4)–C(22)–C(21) 110.1(2), B(2)–N(4)–C(22) 107.5(2), N(3)–B(2)–N(4) 104.6(2), C(16)–B(2)–N(3) 132.6(2), B(2)–N(3)–C(23) 130.4(2), C(21)–N(3)–C(23) 121.2(2), C(16)–B(2)–N(4) 122.7(2), B(2)–C(16)–C(17) 124.4(2), B(2)–C(16)–C(20) 127.2(2), C(17)–C(16)–C(20) 104.8(2).

Fe(1)–C(11) [2.136(2) Å] and Fe(1)–C(16) [2.155(2) Å] contacts are much longer than the remaining Fe–[C(12)–C(15)] [2.042(2)–2.072(2) Å] or Fe–[C(17)–C(20)] [2.026(2)–2.079(2) Å] bonds, although the bond lengths and angles within the heterocycles are similar to those in **3**. As is also the case in **3**, the exocyclic angles N(1)–B(1)–C(11) [132.8(2)°] and N(3)–B(2)–C(16) [132.6(2)°] are more obtuse than the angles N(2)–B(1)–C(11) [122.2(2)°] and N(4)–B(2)–C(16) [122.7(2)°], which reflects the steric requirements of the ferrocene unit.

X-ray Structural Analysis of 15

The molecule of **15** (Figure 3, Table 3) adopts the structure of a three-legged piano-stool with three essentially linear carbonyl ligands. The C–Mn–C angles range from 89.9(2) to 93.6(2)°. The most interesting feature of **15** is the methylcyclopentadienyl ligand, which is linked to a 1,3,2-diazaborolidinyl substituent by a B–C single bond of 1.594(5) Å. The heterocycle is slightly puckered (sum of angles: 532.8°; mean deviation from the best plane: 0.1037 Å), and features a dihedral angle with the cyclopentadienyl ring of 39.6°. The boron atom is located 0.20 Å

above the carbocycle and C(11) is situated 0.44 Å underneath the plane of the heterocycle. The vector B(1)–C(11) forms angles of 7.1° and 13.3° with the carbocycle and the borolidine, respectively.

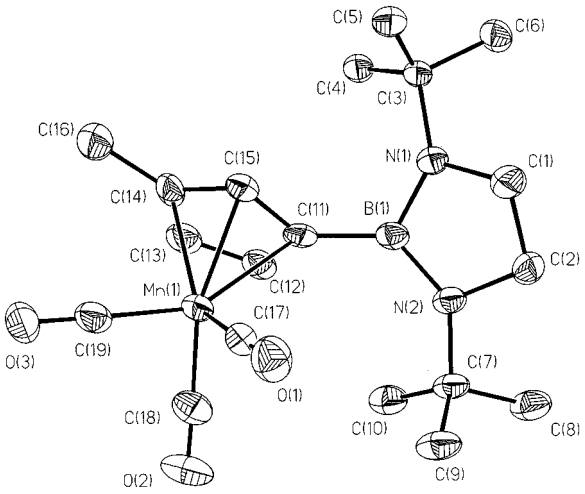

Figure 3. Molecular structure of **15** in the crystal. Selected bond lengths [Å] and angles [°]: B(1)–N(1) 1.445(5), B(1)–N(2) 1.431(5), N(1)–C(1) 1.470(4), N(2)–C(2) 1.469(4), C(1)–C(2) 1.502(5), N(1)–C(3) 1.481(4), N(2)–C(7) 1.489(4), B(1)–C(11) 1.594(5), Mn(1)–C(11) 2.187(3), Mn(1)–C(12) 2.172(4), Mn(1)–C(13) 2.163(4), Mn(1)–C(14) 2.138(4), Mn(1)–C(15) 2.109(3), Mn(1)–C(17) 1.787(4), Mn(1)–C(18) 1.794(4), Mn(1)–C(19) 1.793(4), C–O 1.152(5)–1.156(5); B(1)–N(1)–C(1) 106.8(3), B(1)–N(1)–C(3) 135.4(3), N(1)–C(1)–C(2) 104.1(3), C(1)–N(1)–C(3) 117.8(3), N(2)–C(2)–C(1) 105.5(3), B(1)–N(2)–C(2) 108.2(3), N(1)–B(1)–N(2) 108.2(3), N(1)–B(1)–C(11) 119.7(3), N(2)–B(1)–C(11) 131.7(3), B(1)–C(11)–C(15) 121.4(3), B(1)–C(11)–C(12) 133.9(3), C(12)–C(11)–C(15) 104.1(3), C(17)–Mn(1)–C(18) 93.6(2), C(17)–Mn(1)–C(19) 90.8(2), C(18)–Mn(1)–C(19) 89.9(2), Mn(1)–C–O 177.5(3)–178.9(3).

The manganese atom is unsymmetrically attached to the carbocycle with Mn–C bond lengths ranging from 2.109(3) Å [Mn(1)–C(15)] to 2.187(3) Å [Mn(1)–C(11)]. The B–N distances 1.431(5) and 1.445(5) Å indicate multiple bonding. The remaining endocyclic distances N(1)–C(1) [1.470(4) Å], N(2)–C(2) [1.469(4) Å], and C(1)–C(2) [1.502(5) Å] are single bonds and differ markedly from those in **3** and **6**. The exocyclic angle N(2)–B(1)–C(11) [131.7(3)°] is similar to those of the previously discussed molecules **3** and **6**, and it is wider than the angle N(1)–B(1)–C(11) [119.7(3) Å]. As a consequence of steric hindrance, the exocyclic angles B(1)–N(1)–C(3) [135.4(3)°] and B(1)–N(2)–C(7) [136.7(3)°] clearly exceed the angles C(1)–N(1)–C(3) [117.8(3)°] and C(2)–N(2)–C(7) [115.1(3)°].

Electrochemistry

All the ferrocenyl- and methylcymantrenyl-functionalized diazaboroles and diazaborolidines described here were also investigated by cyclic voltammetry. With the ferrocene derivatives **3**, **6**, **11**, **13**, and **14** a quasi-reversible Fe^{2+}/Fe^{3+} oxidation was observed (Table 2). At low scan rates ($5\ mV\ s^{-1}$) the cyclovoltammograms feature an irreversible wave, which changes to a quasi-reversible one on going to higher rates. The oxidation potentials, $E^{0\prime}$, have been taken from square-wave voltammograms with reference to the redox pair Fc/Fc^+. From these data it is obvious that the diazaborole and the diazaborolidine group transfer electron density onto the redox-active center of the ferrocene unit. The diborolylated ferrocene **6** is more easily oxidized ($E^{0\prime}$ = –0.34 V) than the monoborolylated analog **3** ($E^{0\prime}$ = –0.18 V), and the same trend is observed with compounds **13** ($E^{0\prime}$ = –0.11 V) and **14** ($E^{0\prime}$ = –0.20 V), where one or two diazaborolidinyl substituents are present. Moreover, it is evident that the oxidation of the ferrocenyl-diazaboroles **3** and **6** is easier than the saturated congeners **13** and **14**; no decomposition of the ferrocene derivatives was observed during these experiments. This is not the case with the methylcymantrenyl systems **9** ($E^{0\prime}$ = +0.21 V) and **15** ($E^{0\prime}$ = +0.49 V), where an irreversible oxidation process with the formation of free methylcymantrene ($E^{0\prime}$ = +0.84 V) was observed. Wagner et al. have previously reported that boryl-substituted ferrocenes also suffer from degradation to ferrocene during their cyclovoltammetric studies.[13]

Table 2. Voltammetric data ($E^{0\prime}$) of ferrocenyl- and methylcymantrenyl-functionalized diazaboroles and diazaborolidines vs. Fc/Fc^+ standard.

Compound	**3**	**6**	**9**	**11**	**13**	**14**	**15**
$E^{0\prime}$ [V]	–0.18	–0.34	+0.21	–0.32	–0.11	–0.20	+0.49

Conclusions

We have extended methodologies for the synthesis of 1,3,2-diazaboroles to the construction of ferrocenyl- and cymantrenyl-functionalized diazaboroles. X-ray structure analyses show that the heterocycle is twisted out of the plane of the adjacent cyclopentadienyl ligand in the crystal, thus preventing significant electronic communication by π-electron delocalization. According to the cyclic voltammetric studies, borole and borolidine substituents serve as electron donors and cause cathodic shifts of the oxidation potentials of the iron center relative to the parent system Fc/Fc^+.

Experimental Section

General: All reactions were performed under dry, oxygen-free nitrogen using standard Schlenk techniques. The dibromoboryl derivatives $[(\eta^5\text{-Cp})(\eta^5\text{-}C_5H_4BBr_2)Fe]$ (**1**), $[(\eta^5\text{-}C_5H_4BBr_2)_2Fe]$ (**4**), and $[\{\eta^5\text{-}(3\text{-}CH_3)(1\text{-}Br_2B)C_5H_3\}Mn(CO)_3]$ (**9**), as well as the imines *t*BuN=CH–CH=N*t*Bu[9] and *N*-(2-pyridylmethylene)-*tert*-butylamine,[11] were synthesized as described in the literature. *N*,*N*′-Di-*tert*-butylethane-1,2-diamine and triethylamine were purchased commercially. Infrared spectra were recorded with a Bruker FT-IR IFS 66 spectrometer. NMR spectra: Bruker AM Avance DRX 500. Standards: $SiMe_4$ (^1H, ^{13}C), $BF_3{\cdot}OEt_2$ (^{11}B). Mass spectra were recorded with a VG Autospec sector field mass spectrometer (Micromass). The electrochemical experiments were performed

with a PAR Model 270 A and the relevant software (Model 270). A system of microelectrodes with a three-electrode array was used, with a platinum wire as working electrode (1.5 cm length, 0.5 mm diameter), which was wound as a helix around the counter electrode and a silver wire (1.5 cm length, 1 mm diameter) as pseudo-reference electrode. All experiments were conducted in a glass device, which was flame-dried prior to use and filled with dry nitrogen. The determinations were performed in a 0.1 M solution of tetrabutylammonium hexafluorophosphate (TBAPF) in dichloromethane with concentrations of the analyte of ca. 1×10^{-4} M. The cyclovoltammograms were recorded with scan rates of 5–700 mV s^{-1}. All published potentials were determined by means of square-wave voltammetry (frequency: 5 Hz). Ferrocene and octamethylferrocene were used for calibration. All the potentials with octamethylferrocene were converted into the ferrocene standard.

[(η^5-C_5H_5){η^5-$C_5H_4BN^a$(*t*Bu)CH=CHN^b(*t*Bu)}Fe](*B*–*N*^{b}) (3): Solutions of (dibromoboryl)ferrocene (**1**; 3.10 g, 8.7 mmol) and *N*,*N*′-di-*tert*-butyl-1,4-diazabutadiene (1.46 g, 8.7 mmol), each in *n*-hexane (70 mL), were simultaneously added dropwise to *n*-hexane (50 mL). An olive-green precipitate of borolium salt **2** [^{11}B NMR (CD_3CN): δ = 3.8 and 7.1 ppm] separated. A sample of freshly prepared sodium amalgam (obtained from 1.30 g of Na and 120 g of Hg) was added to the slurry, which was subsequently vigorously stirred in the dark for 2 d. A dark-red solution was decanted and concentrated in vacuo until the solution became cloudy. Storing at –80 °C for 10 d furnished 2.35 g of **3** as red crystals (yield 74%). ^{1}H NMR (C_6D_6): δ = 1.40 (s, 18 H, *t*Bu), 4.10 (s, 5 H, C_5H_5), 4.23 (s, 4 H, C_5H_4B), 6.42 (s, 2 H, NCH) ppm. ^{13}C{^{1}H} NMR (C_6D_6): δ = 32.7 [s, C(*C*H$_3$)$_3$], 53.2 [s, *C*(CH$_3$)$_3$], 68.6 (s, BC$_2{}^a$*C*$_2{}^b$H$_4$), 69.6 (s, C_5H_5), 76.2 (s, BC$_2{}^a$C$_2{}^b$H$_4$), 112.7 (s, NCH) ppm. ^{11}B{^{1}H} NMR (C_6D_6): δ = 25.3 ppm. MS-EI: *m*/*z* (%) = 364 (100) [M$^+$]. $C_{20}H_{29}BFeN_2$ (364.12): calcd. C 65.97, H 8.03, N 7.69; found C 64.78, H. 7.67, N 7.22. Repeated attempts to obtain better analyses were unsuccessful. $E^{0\prime}$ = –0.18 V (vs. Fc/Fc$^+$).

[{η^5-$C_5H_4BN^a$(*t*Bu)CH=CHN^b(*t*Bu)}]Fe(*B*–*N*^{b}) (6): Solutions of 1,1′-Bis(dibromoboryl)ferrocene (**4**; 2.20 g, 6.2 mmol) and *N*,*N*′-di-*tert*-butyl-1,4-diazabutadiene (2.09 g, 12.4 mmol), each in *n*-hexane (70 mL), were simultaneously added dropwise to *n*-hexane (25 mL), whereby the olive-green borolium salt **5** (^{11}B{^{1}H} NMR: δ = 3.8, 7.1 ppm) separated. Freshly prepared sodium amalgam (obtained from 1.30 g of Na and 120 g of Hg) was added, and the slurry was vigorously stirred in the dark for 2 d. A dark-red solution was decanted from the mercury phase and concentrated in vacuo until the solution turned cloudy. Storing of the solution at –80 °C for 12 d and then at –10 °C for 2 d gave 2.72 g (81% yield) of compound **6** as cherry-red crystals. ^{1}H NMR (C_6D_6): δ = 1.42 (s, 36 H, *t*Bu), 4.23 (s, 4 H, Cp), 4.36 (s, 4 H, Cp), 6.39 (s, 4 H, NCH) ppm. ^{13}C{^{1}H} NMR (C_6D_6): δ = 32.8 [s, C(*C*H$_3$)$_3$], 53.2 [s, *C*(CH$_3$)$_3$], 69.2 (s, CH-Cp), 79.3 (s, CH-Cp), 112.9 (s, NCH) ppm. ^{11}B{^{1}H} NMR (C_6D_6): δ = 25.3 ppm. MS-EI: *m*/*z* (%) = 542 (100) [M$^+$]. $C_{30}H_{48}BFeN_2$ (542.21): calcd. C 66.46, H 8.92, N 10.33; found C 66.53, H 9.12, N 9.90. $E^{0\prime}$ = –0.34 V (vs. Fc/Fc$^+$).

[{(3-Me)[1-BN^a(*t*Bu)CH=CHN^b(*t*Bu)]C_5H_3}Mn(CO)$_3$](*B*–*N*^{b}) (9): Solutions of 1-dibromoboryl-3-methylcymantrene (**7**; 4.00 g, 10.3 mmol) and *N*,*N*′-di-*tert*-butyl-1,4-diazabutadiene (1.74 g, 10.3 mmol), each in *n*-hexane (100 mL), were slowly added (one drop per second!) to *n*-hexane (50 mL). The dark-yellow borolium salt **8** [^{11}B{^{1}H} NMR (CD_3CN): δ = 5.0 ppm] separated. It was filtered and washed with *n*-hexane (3 × 40 mL). The salt was suspended in *n*-hexane (100 mL), sodium amalgam (from 1.60 g of Na and 165 g of Hg) was added, and the resulting slurry was vigorously stirred in the dark for 2 d. Storing at –30 °C for 4 d gave yellow crystals of thermolabile **9** (2.58 g, 63%). Decomposition at room temp. was complete after 24 h. ^{1}H NMR (C_6D_6): δ = 1.34 (s, 18 H, *t*Bu), 1.56 (s, 3 H, CH_3), 4.04 (s, 1 H, C_5H_3), 4.57 (s, 1 H, C_5H_3), 4.65 (s, 1 H, C_5H_3), 6.34 (s, 2 H, NCH) ppm. ^{13}C{^{1}H} NMR (C_6D_6): δ = 12.8 (s, CH_3), 32.9 [s, C(*C*H$_3$)$_3$], 53.6 [s, *C*(CH$_3$)$_3$], 82.1 (s, C4), 94.4; 95.2 (2s, C2, C5), 99.8 (s, C3), 113.7 (s, NCH), 226.2 (s, CO) ppm. ^{11}B{^{1}H} NMR (C_6D_6): δ = 23.2 (s) ppm. MS-EI: *m*/*z* (%) = 396 (21) [M$^+$], 312 (63) [M$^+$ – 3CO], 296 (100) [M$^+$ – 3CO – CH_4]. $C_{19}H_{26}BMnN_2O_3$ (396.18): calcd. C 57.60, H 6.61, N 7.07; found C 57.09, H 6.87, N 7.08. $E^{0\prime}$ = +0.21 V (vs. Fc/Fc$^+$).

[*t*BuN^aC^{b}H=C^{c}C^{d}H=C^{e}HC^{f}H=C^{g}HN^hBC_5H_4](C_5H_5)Fe(*N*^{a}–*B*,*N*^{h}–*C*^{e}) (11): Solutions of (dibromoboryl)ferrocene (**1**; 1.70 g, 4.78 mmol) and *N*-(2-pyridylmethylene)-*tert*-butylamine (0.70 g, 4.78 mmol), each in *n*-hexane (20 mL), were simultaneously added dropwise to *n*-hexane (50 mL). Stirring for 4 h led to the precipitation of borolium salt **10** as an olive-green solid [^{11}B{^{1}H} NMR (CD_3CN): δ = 6.3, 7.8 ppm]. Sodium amalgam (obtained from 0.23 g of Na and 213 g of Hg) was added and the suspension was stirred in the dark for 3 d. The *n*-hexane phase was decanted and concentrated until the beginning of cloudiness. Storing at –80 °C for 2 d gave 1.16 g (68% yield) of **11** as an orange solid. ^{1}H NMR (C_6D_6): δ = 1.35 (s, 9 H, *t*Bu), 4.00 (s, 5 H, C_5H_5), 4.21 (s, 2 H, C_5H_4), 4.31 (s, 2 H, C_5H_4), 5.78 (m, 1 H, CH), 6.16 (m, 1 H, CH), 6.47 (s, 1 H, *t*BuNC*H*), 6.78 (m, 1 H, CH), 8.33 (s, 1 H, CH) ppm. ^{13}C{^{1}H} NMR (C_6D_6): δ = 32.6 [s, C(*C*H$_3$)$_3$], 53.7 [s, *C*(CH$_3$)$_3$], 68.0 (s, C_5H_4), 68.7 (s, C_5H_5), 69.7 (s, C_5H_4), 74.4(s, C_5H_4), 105.1 (s, *t*BuN*C*H), 105.7 (s, CH), 117.7 (s, CH), 119.0 (s, CH), 126.6 (s, *t*BuNCH=*C*), 130.9 (s, CH) ppm. ^{11}B{^{1}H} NMR (C_6D_6): δ = 23.9 ppm. MS-EI: *m*/*z* (%)= 318 (9) [M$^+$ – 2 CH_3]. $C_{20}H_{23}BFeN_2$ (358.09): calcd. C 67.08, H 6.47, N 7.82; because of the thermolability of **11** no reliable elemental analyses could be obtained. $E^{0\prime}$ = –0.32 V (vs. Fc/Fc$^+$).

[{η^5-$C_5H_4BN^a$(*t*Bu)$CH_2CH_2N^b$(*t*Bu)}(η^5-C_5H_5)Fe](*B*–*N*^{b}) (13): A solution of **1** (2.80 g, 7.8 mmol) in *n*-hexane (10 mL) was added to a chilled (0 °C) solution of NEt_3 (1.60 g, 15.6 mmol) in *n*-hexane (50 mL). It was warmed to room temp., 1.40 g (8.00 mmol) of neat *N*,*N*′-di-*tert*-butylethane-1,2-diamine was added dropwise, and the mixture was heated under reflux for 3 h. It was then filtered and the filtrate was concentrated to dryness. Distillation of the residue at 250 °C and 10^{-6} bar afforded 2.46 g (86%) of product **13** as a red oil (b.p. 210 °C, 10^{-6} bar). ^{1}H NMR (C_6D_6): δ = 1.26 (s, 18 H, *t*Bu), 3.11 (s, 4 H, NCH_2), 4.08 (s, 5 H, C_5H_5), 4.18 (s, 2 H) and 4.19 (s, 2 H, C_5H_4B) ppm. ^{13}C{^{1}H} NMR (C_6D_6): δ = 31.3 [s, C(*C*H$_3$)$_3$], 45.5 (s, NCH_2), 51.7 [s, *C*(CH$_3$)$_3$], 68.3 (s) and 76.2 (s, C_5H_4B), 69.6 (s, C_5H_5) ppm. ^{11}B{^{1}H} NMR (C_6D_6): δ = 31.8 ppm. MS-EI: *m*/*z* (%) = 366 (63) [M$^+$], 351 (20) [M$^+$ – CH_3], 294 (31) [M$^+$ – *t*Bu – H$^+$]. $C_{20}H_{31}BFeN_2$ (366.64): calcd. C 65.46, H 8.51, N 7.63; found C 64.82, H 8.69, N 7.40. $E^{0\prime}$ = –0.11 V (vs. Fc/Fc$^+$).

[{$C_5H_4BN^a$(*t*Bu)$CH_2CH_2N^b$(*t*Bu)}$_2$Fe](*B*–*N*$_b$) (14): A solution of **4** (4.00 g, 7.6 mmol) in *n*-hexane (40 mL) was added dropwise to a chilled (0 °C) solution of Et_3N (3.08 g, 30.4 mmol) in *n*-hexane (100 mL). The mixture was then warmed to room temp., combined with neat *N*,*N*′-di-*tert*-butylethane-1,2-diamine (2.63 g, 15.2 mmol), and heated under reflux for 4 h. It was then filtered and the filtrate concentrated to dryness. The deep-red solid residue was dissolved in *n*-hexane (20 mL), and the solution was stored at –80 °C for 7 d to give 3.62 g (87% yield) of red solid **14**. ^{1}H NMR (C_6D_6): δ = 1.43 (s, 18 H, *t*Bu), 3.23 (s, 8 H, NCH_2), 4.30 and 4.44 (m, 8 H, C_5H_4B) ppm. ^{13}C{^{1}H} NMR (C_6D_6): δ = 31.4 [C(*C*H$_3$)$_3$], 45.5 (s, NCH_2), 51.8 [s, *C*(CH$_3$)$_3$], 68.9 [s, C(3),(4)], 79.0 [s, C(2),(5)] ppm. ^{11}B{^{1}H} NMR (C_6D_6): δ = 31.8 ppm. MS-EI: *m*/*z* (%) = 546

Table 3. Crystallographic data for **3**, **6**, and **15**.

	3	**6**	**15**
Empirical formula	$C_{20}H_{29}BFeN_2$	$C_{30}H_{48}B_2FeN_4$	$C_{19}H_{28}BMnN_2O_3$
Color	red	orange	colorless
Size [mm]	0.24 × 0.20 × 0.17	0.21 × 0.14 × 0.06	0.15 × 0.07 × 0.06
M_r	364.11	542.19	398.18
Crystal system	orthorhombic	triclinic	triclinic
Space group	$P2_12_12_1$	$P\bar{1}$	$P\bar{1}$
a [Å]	9.3010(2)	10.6860(2)	9.0730(9)
b [Å]	10.7800(2)	11.8430(3)	10.5250(7)
c [Å]	18.4140(3)	13.2840(4)	11.5870(12)
α [°]	90	108.3010(15)	82.936(6)
β [°]	90	93.1290(17)	88.844(6)
γ [°]	90	112.0801(15)	65.658(5)
V [Å^3]	1846.28(6)	1450.30(6)	999.89(16)
$\rho_{calcd.}$ [g cm^{-3}]	1.310	1.242	1.323
Z	4	2	2
F(000)	776	584	420
μ [mm^{-1}]	0.820	0.546	0.680
Θ [°]	3.10–27.5	2.91–27.45	2.95–25.00
T [K]	100	100	100
Refl. measured	24538	37733	9676
Unique refl.	4206	6599	3509
R(int)	0.049	0.086	0.061
No refl. [$I > 2\sigma(I)$]	3949	4865	2689
Refined parameters	223	346	242
R_F [$I > 2\sigma(I)$]	0.0244	0.0474	0.0540
wR_F^2 [$I > 2\sigma(I)$]	0.0584	0.1014	0.1373
$\Delta\rho_{max./min.}$ [e Å^{-3}]	0.259/–0.278	0.394/–0.274	0.935/–0.661
CCDC-	273089	273090	273091

(100) [M$^+$], 490 (10) [M$^+$ – $Me_2C{=}CH_2$]. $C_{30}H_{52}BFeN_4$ (546.26): calcd. C 65.97, H 9.59, N 10.26; found C 65.97, H 9.64, N 9.98. $E^{0\prime}$ = –0.20 V (vs. Fc/Fc$^+$).

[{(3-Me)[1-BN^a(*t*Bu)CH$_2$CH$_2$N^b(*t*Bu)][C$_5$H$_3$}Mn(CO)$_3$](*B*–*N*^{b}) (15): A sample of neat **7** (5.30 g, 13.6 mmol) was combined with a chilled (0 °C) solution of Et_3N (2.80 g, 27.1 mmol) in *n*-hexane (100 mL), whereby a colorless precipitate separated. It was warmed to room temp. and 2.30 g (27.1 mmol) of neat *N*,*N*′-di-*tert*-butylethane-1,2-diamine was added dropwise. This mixture was heated under reflux for 3 h. After filtration, the filtrate was freed from solvent and the yellow oily residue was distilled at 10^{-6} bar and 150 °C bath temperature. The distillate was dissolved in *n*-pentane (40 mL) and stored at –30 °C for 7 d to afford crystalline **15** (yield: 4.60 g, 85%). ^{1}H NMR (C_6D_6): δ = 1.30 (s, 18 H, *t*Bu), 1.68 (s, 3 H, CH_3), 3.11 (s, 4 H, CH_2), 4.14 [s, 1 H, H(4)], 4.63 and 4.68 [s, 2 H, H(2),(5)] ppm. ^{13}C{^{1}H} NMR (C_6D_6): δ = 12.8 (s, CH_3), 31.2 [s, C(CH_3)$_3$], 45.3 (s, NCH_2), 51.9 [s, $C(CH_3)_3$], 81.7 [s, C(4)], 93.5 and 94.1 [2 s, C(2),(5)], 99.8 [s, C(3)], 226.0 (s, CO) ppm. ^{11}B{^{1}H} NMR (C_6D_6): δ = 29.6 ppm. IR (KBr): $\tilde{\nu}$ = 2009 cm^{-1} (s, CO), 1908 (br. s, CO). MS-EI: *m*/*z* (%) = 398 (10) [M$^+$], 314 (85) [M$^+$ – 3 CO], 298 (100) [M$^+$ – 3 CO – CH_4]. $C_{19}H_{28}BN_2MnO_3$ (398.19): calcd. C 57.31, H 7.09, N 7.04; found C 56.94, H 6.88, N 6.71. $E^{0\prime}$ = +0.49 V (vs. Fc/Fc$^+$). CCDC-273089 to -273091 contain the supplementary crystallographic data for this paper. These data can be obtained free of charge via www.ccdc.cam.ac.uk/data_request/cif (see also Table 3).

[1] S. Aldridge, C. Bresner, *Coord. Chem. Rev.* **2003**, *244*, 71–92.
[2] K. Ma, M. Scheibitz, S. Scholz, M. Wagner, *J. Organomet. Chem.* **2002**, *652*, 11–19.
[3] Review: L. Weber, *Coord. Chem. Rev.* **2001**, *215*, 39–77.
[4] a) L. Weber, E. Dobbert, A. Rausch, H.-G. Stammler, B. Neumann, *Z. Naturforsch., Teil B* **1999**, *54*, 363–371; b) L. Weber, E. Dobbert, H.-G. Stammler, R. Boese, D. Bläser, *Eur. J. Inorg. Chem.* **1999**, 491–497; c) L. Weber, E. Dobbert, R. Boese, M. T. Kirchner, D. Bläser, *Eur. J. Inorg. Chem.* **1998**, 1145–1152; d) L. Weber, E. Dobbert, H.-G. Stammler, B. Neumann, R. Boese, D. Bläser, *Chem. Ber./Recueil* **1997**, *130*, 705–710.
[5] a) L. Weber, M. Schnieder, T. C. Maciel, H. Wartig, M. Schimmel, R. Boese, D. Bläser, *Organometallics* **2000**, *19*, 5791–5794; b) L. Weber, A. Rausch, H.-G. Stammler, B. Neumann, *Z. Anorg. Allg. Chem.* **2005**, *631*, 1633–1639.
[6] a) J. S. Merriam, K. Niedenzu, *J. Organomet. Chem.* **1973**, *51*, C1–C2; b) K. Niedenzu, J. S. Merriam, *Z. Anorg. Allg. Chem.* **1974**, *406*, 251–259; c) G. Schmid, M. Polk, R. Boese, *Inorg. Chem.* **1990**, *29*, 4421–4429.
[7] a) L. Weber, G. Schmid, *Angew. Chem.* **1974**, *86*, 519; *Angew. Chem. Int. Ed. Engl.* **1974**, *13*, 467; b) G. Schmid, J. Schulze, *Chem. Ber.* **1977**, *110*, 2744–2750.
[8] a) N. Ruf, T. Renk, W. Siebert, *Z. Naturforsch., Teil B* **1976**, *31*, 1028–1034; b) T. Renk, W. Ruf, W. Siebert, *J. Organomet. Chem.* **1976**, *120*, 1–25.
[9] J. M. Klugman, R. K. Barnes, *Tetrahedron* **1970**, *26*, 2555–2560.
[10] I. Domke, L. Weber, unpublished results.
[11] A. J. Clark, D. J. Duncalf, R. P. Filik, D. W. Haddleton, G. H. Thomas, H. Wongtap, *Tetrahedron Lett.* **1999**, *40*, 3807.
[12] M. Herberhold, U. Dörfler, B. Wrackmeyer, *Polyhedron* **1995**, *14*, 2683–2689.
[13] a) M. Fontani, F. Peters, W. Scherer, W. Wachter, M. Wagner, P. Zanello, *Eur. J. Inorg. Chem.* **1998**, 1453–1465; b) K. Ma, H.-W. Lerner, S. Scholz, J. W. Bats, M. Bolte, M. Wagner, *J. Organomet. Chem.* **2002**, *664*, 94–105.

Received: June 2, 2005
Published Online: October 13, 2005

